Inorganic Chemistry

Article

pubs.acs.org/IC

Synthesis and Characterization of *N*-[2-P(*i*-Pr)$_2$-4-methylphenyl]$_2^-$ (PNP) Pincer Tin(IV) and Tin(II) Complexes

Jens Henning,[†] Hartmut Schubert,[†] Klaus Eichele,[†] Florian Winter,[‡] Rainer Pöttgen,[‡] Hermann A. Mayer,[†] and Lars Wesemann*[,†]

[†]Institut für Anorganische Chemie, Universität Tübingen, Auf der Morgenstelle 18, D-72076 Tübingen, Germany

[‡]Institut für Anorganische und Analytische Chemie, Universität Münster, Corrensstrasse 30, D-48149 Münster, Germany

Supporting Information

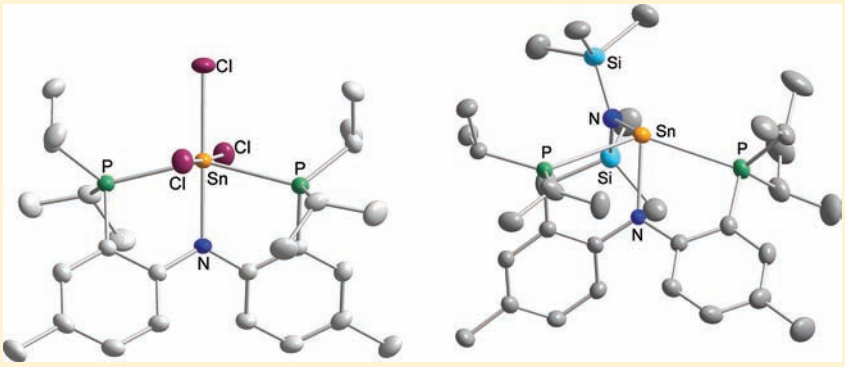

ABSTRACT: *N*-[2-P(*i*-Pr)$_2$-4-methylphenyl]$_2^-$ (PNP) pincer complexes of tin(IV) and tin(II), [(PNP)SnCl$_3$] (**2**) and [(PNP)SnN(SiMe$_3$)$_2$] (**3**), respectively, were prepared and characterized by X-ray diffraction, solution and solid state NMR spectroscopy, and ^{119}Sn Mössbauer spectroscopy. Furthermore, ^{119}Sn cross polarization magic angle spinning NMR spectroscopic data of [Sn(NMe$_2$)$_2$]$_2$ are reported. Compound **2** is surprisingly stable toward air, but attempts to substitute chloride ligands caused decomposition.

INTRODUCTION

In recent years, many endeavors in the field of anionic[1−7] and neutral[8] pincer ligand chemistry were undertaken. A widespread group of anionic *N*-[2-P(*i*-Pr)$_2$-4-methylphenyl]$_2^-$ (PNP) type ligands, which came up in 2003, contains the bis-*o*-aryl backbone as linkage between the coordinating atoms phosphorus and nitrogen.[9,10] Complexes of most transition metals have been prepared by now, some of them exhibiting unusual reactivity.[11−23] For instance, the group of Mindiola reported the C−H bond activation of benzene by a titanium alkylidyne fragment containing the bis[2-(di-*iso*-propylphosphino)-4-methylphenyl]amido ligand (PNP).[11,24,25]

However, at the beginning of our work, very few main group metal complexes of PNP ligands were reported. Indeed, merely those of lithium, aluminum, and thallium were known.[12,23,26,27] By now, complexes of gallium and indium have been prepared as well.[28] In analogy to the surprising reactivity of the above-mentioned titanium complex containing a group 4 metal, we wondered if group 14 metal complexes of the PNP ligand are accessible and which reactivity they might show. It has to be mentioned that pincer complexes of group 14 metals have been prepared previously but with pincer ligands not containing phosphorus as donating atoms.[29−33]

Herein we report the preparation and characterization of the novel PNP tin complexes [(PNP)SnCl$_3$] (**2**) and [(PNP)SnN(SiMe$_3$)$_2$] (**3**), containing tin(IV) and tin(II), respectively. In addition, we present ^{31}P and ^{119}Sn NMR spectroscopic data of [(PNP)SnNMe$_2$] (**4**) providing insight into tin−phosphorus bonding.

RESULTS AND DISCUSSION

The tin(IV) complex **2** was obtained readily by the reaction of SnCl$_4$ with 1 equiv of the lithium salt of PNP (**1**) as orange powder in 78% yield (Scheme 1). The product is surprisingly inert toward air, and we expected it to be a good starting material for further substitution of the chloride ligands. So far reactions of the trichloride **2** with several alkylating and hydride reagents (e.g., AlMe$_3$, EtMgBr, LiAlH$_4$) resulted in decomposition of the tin moiety yielding the protonated ligand H(PNP). Considering that, we assume a significant weakening of the bonding interaction of the tin atom to the pincer ligand caused by the substitution of the electron withdrawing chloride ligands by electron donating alkyl or hydrido ligands. Thus, decomposition occurs, despite the chelating properties of the (PNP) ligand.

The yellow divalent tin[34] complex **3** was obtained in 60% yield by reacting the lithium salt **1** with 1 equiv of the

Received: February 13, 2012
Published: April 30, 2012

   dx.doi.org/10.1021/ic300324s | *Inorg. Chem.* 2012, 51, 5787−5794

Scheme 1

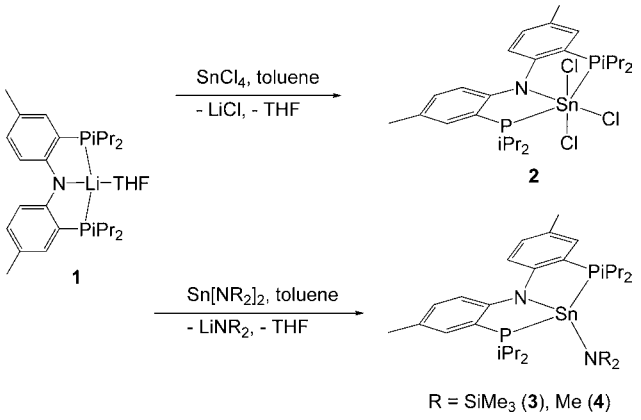

stannylene $Sn[N(SiMe_3)_2]_2$. The reaction product **3** is much more sensitive than the tin(IV) complex and has to be stored under inert gas.

Using the tin(II) derivative $Sn[NMe_2]_2$ as starting material for the reaction with the ligand **1** leads to a product that shows a quite similar $^{31}P\{^1H\}$ NMR spectrum compared to compound **3** (vide infra). Considering this and the analogy of the synthesis of compound **3**, we assume that an analogous complex is built with an $[NMe_2]^-$ ligand instead of the $[N(SiMe_3)_2]^-$ ligand. Unfortunately, [(PNP)SnNMe$_2$] (**4**) seems to be even more sensitive than compound **3**, so we were not able to isolate a sample for a proper elemental analysis.

X-ray Diffraction. Red orange block shaped single crystals of the tin derivative **2** were grown in good yield from a dichloromethane solution of the crude product by slow diffusion of diethylether into it. Compound **2** crystallizes in the space group *P*2/*c* with half of the molecule in the asymmetric unit.

The molecular structure of the tin(IV) complex **2** (Figure 1) shows C_2 symmetry with Cl(2), Sn(1), and N(1) lying on the axis of symmetry. The coordination geometry of the tin atom is distorted octahedral. The [P(1)−Sn(1)−P(1)*] angle is compressed [152.81(2)°], while all other angles are in good agreement with the ideal octahedral geometry. The Sn(1)−N(1) distance [2.157(2) Å] lies within the upper range of reported Sn−N bond lengths of tin amides [1.980(4)−2.1649(12) Å].[35−41] Caused by the C_2 axis of the molecule, the angles around N(1) perfectly add up to 360° indicating planarity.

The Sn(1)−P(1) distance [2.5739(5) Å] is fractionally shorter than in the structural akin complexes *trans*-$[SnCl_4(PEt_3)_2]$ [2.615(5) Å] and $\{SnCl_4[Et_2P(CH_2)_2PEt_2]\}$ [2.6481(17) Å].[42,43] The Sn(1)−Cl(2) bond [2.4069(7) Å] trans to the nitrogen atom is a little shorter than the Sn(1)−Cl(1) bond [2.4430(5) Å] cis to it. Both compare well to the Sn−Cl distances in the aforementioned complexes [2.4084(14)−2.455(5) Å].[42,43] In the solid state short Cl−H distances are observed between Cl(1) and two of the *iso*-propyl hydrogen atoms, one on each side. The distances of 2.59 Å and 2.67 Å are shorter than the van der Waals distance of 2.95 Å.

Bright yellow single crystals of complex **3** were obtained by slow evaporation of a toluene or hexane solution of the product. Compound **3** crystallizes in the space group $P\bar{1}$ (Figure 2). The coordination geometry around the tin atom is irregular. The [P(1)−Sn(1)−P(2)] angle [141.41(2)°] is about

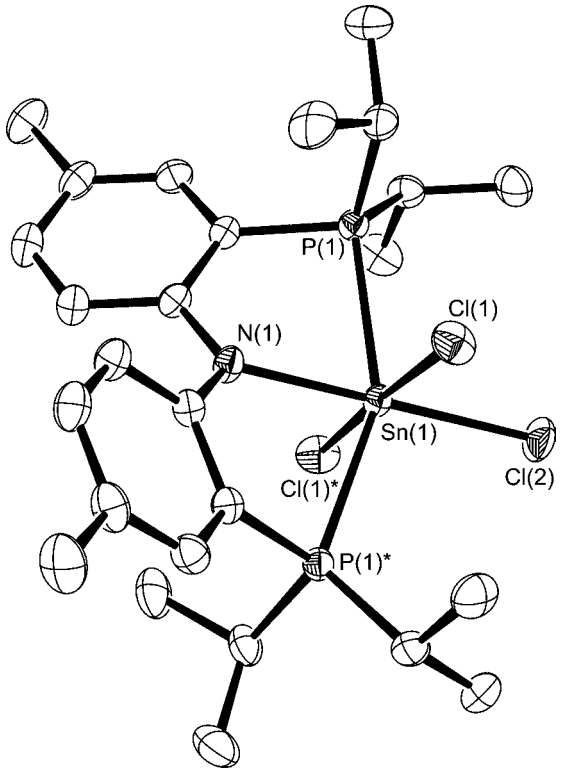

Figure 1. ORTEP plot (50% probability level) of the molecular structure of **2** in the solid state. All hydrogen atoms are omitted for the sake of clarity. Selected bond lengths [Å] and angles [°]: Sn(1)−N(1) 2.157(2), Sn(1)−P(1) 2.5739(5), Sn(1)−Cl(1) 2.4430(5), Sn(1)−Cl(2) 2.4069(7), P(1)−Sn(1)−P(1)* 152.81(2), Cl(1)−Sn(1)−Cl(2) 88.392(13), Sn(1)−N(1)−C(1) 118.47(11), C(1)−N(1)−C(1)* 123.1(2).

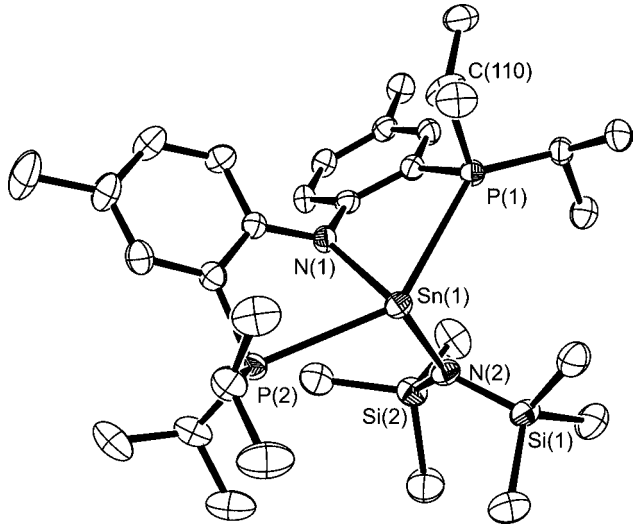

Figure 2. ORTEP plot (50% probability level) of the molecular structure of **3**. The *iso*-propyl group at C(110) is 2-fold disordered with only one position being displayed here. All hydrogen atoms are omitted for the sake of clarity. Selected bond lengths [Å] and angles [°]: Sn(1)−N(1) 2.206(2), Sn(1)−N(2) 2.142(2), Sn(1)−P(2) 2.8820(7), Sn(1)−P(1) 2.9698(7), N(1)−Sn(1)−N(2) 101.56(9), P(1)−Sn(1)−P(2) 141.41(2), Sn(1)−N(1)−C(1) 123.95(16), Sn(1)−N(1)−C(8) 118.34(16), C(1)−N(1)−C(8) 116.9(2), Sn(1)−N(2)−Si(1) 110.68(12), Sn(1)−N(2)−Si(2) 128.36(13), Si(1)−N(2)−Si(2) 120.77(13).

dx.doi.org/10.1021/ic300324s | *Inorg. Chem.* 2012, 51, 5787−5794

11.4° smaller than in complex **2**. Considering the rigidity of the ligand the more compressed angle is in agreement with the longer Sn−P [Sn(1)−P(1), 2.8820(7) Å and Sn(1)−P(2), 2.9698(7) Å] and Sn−N bonds [Sn(1)−N(1), 2.206(2) Å]. Also the [N(1)−Sn(1)−N(2)] angle of 101.56(9)° is small in accordance with the VSEPR theory assigning the major sterical demand to the lone pair. The meridional coordination geometry of the pincer ligand is slightly distorted, too, indicated by the angle of 11.36(11)° between the planes [P(1)−N(1)−Sn(1)] and [P(2)−N(1)−Sn(1)]. The rigidity of the PNP ligand as well gives rise to the considerably longer Sn(1)−N distance to the pincer nitrogen atom N(1) in comparison to the silazide nitrogen atom [Sn(1)−N(2), 2.142(2) Å]. For the latter some examples of tin(II) hexamethyldisilazides with similar distances have been reported [2.144(5) and 2.147(3) Å],[44,45] and an example of a tin(IV) amide with an even longer Sn−N distance of 2.221(5) Å is known.[46] The angles around N(1) and N(2) add up to 359.2(5)° and 359.8(4)° indicating planarity for both nitrogen atoms.

The Sn−P bond lengths [Sn(1)−P(1), 2.8820(7) Å and Sn(1)−P(2), 2.9698(7) Å] are by 0.308 and 0.396 Å longer than in complex **2** and in the literature only very few examples of similar or longer Sn−P distances can be found (up to 3.078 Å).[47−51]

Solution NMR Spectroscopy. In agreement with the C_2 symmetry of the molecular structure of tin complex **2** the $^{31}P\{^1H\}$ NMR spectrum shows one singlet at −7.0 ppm (CD_2Cl_2) exhibiting tin satellites (natural abundances: ^{119}Sn 8.59%, ^{117}Sn 7.68%, ^{115}Sn 0.34%) with $^1J(^{119}Sn-^{31}P)$ = 1672 Hz, $^1J(^{117}Sn-^{31}P)$ = 1597 Hz, and $^1J(^{115}Sn-^{31}P)$ = 1466 Hz. Accordingly, the $^{119}Sn\{^1H\}$ NMR spectrum reveals a triplet at −500 ppm with a $^1J(^{119}Sn-^{31}P)$ coupling constant of 1672 Hz. The $^1J(^{119}Sn-^{31}P)$ coupling constant lies between the coupling constants of the complexes *trans*-$[SnCl_4(PEt_3)_2]$ and $\{SnCl_4[Et_2P(CH_2)_2PEt_2]\}$. The trans complex has significant greater and the cis complex a significant smaller $^1J(^{119}Sn-^{31}P)$ coupling constant of 2383 and 1049 Hz, respectively.[42,43]

As expected from the molecular structure of the stannylene **3** solution $^{31}P\{^1H\}$ NMR spectroscopy exhibits two chemically inequivalent phosphorus signals at −14.5 ppm and −1.9 ppm, appearing as doublets with a $^2J(^{31}P-^{31}P)$ coupling constant of 160 Hz, which lies within the higher end of reported $^2J(^{31}P-^{31}P)$ coupling constants of tin complexes (88−162 Hz).[52] Each of the doublets carries diagnostic tin satellites. The coupling constants are given in Table 1. In agreement with the $^{31}P\{^1H\}$ NMR data, the $^{119}Sn\{^1H\}$ NMR spectrum gives rise to one signal at −177 ppm which is composed of a doublet of doublets with $^1J(^{119}Sn-^{31}P)$ coupling constants of 978 and 585 Hz.

Table 1. $^{31}P\{^1H\}$ and $^{119}Sn\{^1H\}$ NMR Data of 2−4[a]

	$\delta(^{31}P)$	$\delta(^{119}Sn)$	$^2J(^{31}P,^{31}P)$	$^1J(^{119}Sn,^{31}P)$	$^1J(^{117}Sn,^{31}P)$	spin system
2	−7.0	−500		1672	1597	A_2X
3	−14.5	−177	160	585	548	AMX
	−1.9			978	931	
4	−8.5	−151	150	(±)382	(±)365	ABX
	−5.0			(±)941	(±)899	

[a]Chemical shift values are given in ppm and coupling constants are in Hz.

In addition the $^{31}P\{^1H\}$ and $^{119}Sn\{^1H\}$ NMR spectroscopic data of compound **4** reveal an interesting insight into the tin−phosphine bond. The signal patterns in both spectra are similar to those of the tin(II) complex **3**. In contrast they have to be treated as higher order spectra because of the smaller chemical shift difference of the two phosphorus signals at −8.5 ppm and −5.0 ppm (Figure 3). The $^{119}Sn\{^1H\}$ NMR spectrum shows a multiplet at −151 ppm. Simulation of the ABX spectra affords the P−P and Sn−P coupling constants given in Table 1.[53] The simulation also allowed determination of the relative algebraic signs of the AX and BX coupling constants as being equal.

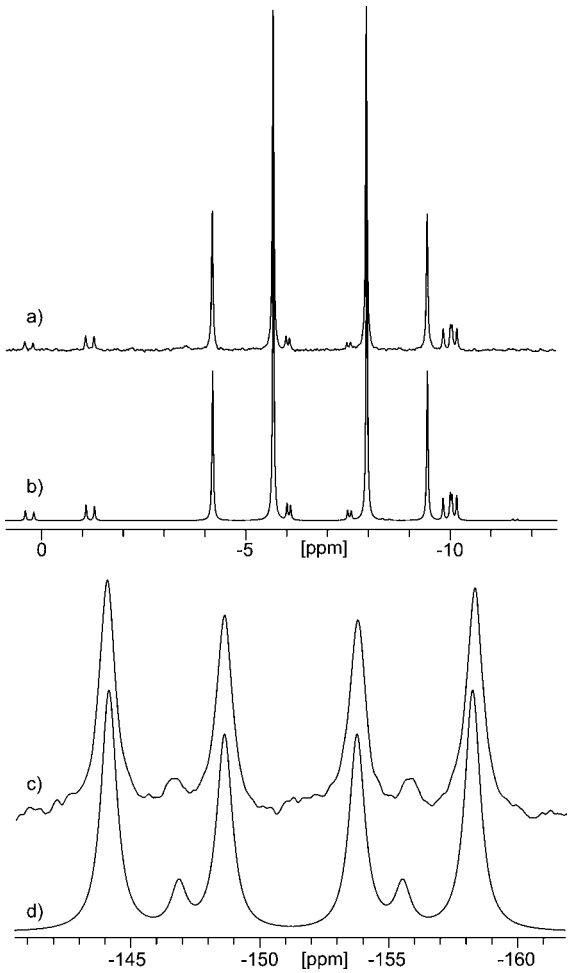

Figure 3. Measured (a, c) and simulated (b, d) $^{31}P\{^1H\}$ NMR (top) and $^{119}Sn\{^1H\}$ NMR (bottom) spectra of compound **4**.

The tin−phosphorus coupling constants show significantly smaller values for the tin(II) complexes **3** and **4** than for the tin(IV) complex **2**; this might be interpreted as an indicator for weaker bonding of the phosphines to the bivalent tin atoms. This matches the expectations due to the higher Lewis acidity of the tin atom in compound **2** arising from the tetravalent configuration and the electron withdrawing chloride ligands.

An interesting observation is the inequality of the two phosphorus atoms in each of the tin(II) complexes even in solution NMR spectroscopy at elevated temperatures (60 °C).

For both compounds **3** and **4**, the $^1J(^{119}Sn-^{31}P)$ coupling constants of the signals at higher frequencies are quite similar at about 950 Hz, whereas the signals at lower frequencies show considerably smaller coupling constants (**3**, 585 Hz; **4**, 382 Hz).

dx.doi.org/10.1021/ic300324s | *Inorg. Chem.* 2012, 51, 5787−5794

Remarkable are the changes in the NMR spectroscopic data that arise from the substitution of the $[N(SiMe_3)_2]^-$ ligand (**3**) by $[NMe_2]^-$ (**4**): Both $^1J(^{119}Sn-^{31}P)$ coupling constants of derivative **4** are smaller than the corresponding coupling constants of derivative **3**. And the difference between the two tin−phosphorus coupling constants of compound **4** (559 Hz) is considerably larger than that of compound **3** (303 Hz) while the difference of the chemical shifts is smaller for compound **4**.

Solid State NMR Spectroscopy. In order to bridge the gap between crystal structures in the solid state and NMR experiments in solution, we have also obtained ^{31}P and ^{119}Sn cross-polarization magic-angle spinning (CP/MAS) solid-state NMR spectra of **2**, **3** and the starting materials H(PNP) and $[Sn(NMe_2)_2]_2$. The results on these compounds as well as data on related systems from the literature are collected in Tables 2 and 3.

Table 2. Principal Components[a] of the ^{31}P NMR Chemical Shift Tensors of Compounds 2, 3, H(PNP) and Examples from the Literature

compound	δ_{iso}/ppm	δ_{11}/ ppm	δ_{22}/ ppm	δ_{33}/ ppm	Ω/ ppm	κ
H(PNP)	−15.0	24	−2	−67	91	0.43
	−19.5	20	−5	−73	93	0.47
(PNP)$SnCl_3$, **2**	−10.5[b]	34	6	−72	106	0.48
(PNP) $SnN(SiMe_3)_2$, **3**	−10.2[c,d]	27	0	−58	85	0.35
	−13.4[d,e]	22	−13	−48	70	0.00
PPh_3	−10[f]	9	9	−42	51	1.00
$PPhCy_2$	3[f]	38	3	−32	70	0.00
PCy_3	7[f]	35	18	−30	65	0.48
PPh_2iPr	−3[f]	26	6	−41	67	0.40
$PPh_2(2\text{-}MeC_6H_4)$	−17[f]	15	−28	−38	53	−0.62

[a] $\delta_{11} \geq \delta_{22} \geq \delta_{33}$, isotropic chemical shift $\delta_{iso} = (\delta_{11} + \delta_{22} + \delta_{33})/3$, span $\Omega \approx \delta_{11} - \delta_{33}$, skew $\kappa = 3(\delta_{22} - \delta_{iso})/\Omega$; $-1 \leq \kappa \leq 1$. [b] $^1J(^{117,119}Sn,^{31}P)$ = 1568 Hz. [c] $^1J(^{117,119}Sn,^{31}P)$ = 500 Hz. [d] $^2J(^{31}P,^{31}P)$ = 211 Hz. [e] $^1J(^{117,119}Sn,^{31}P)$ = 650 Hz. [f] Ref 71.

The crystal structure of the free H(PNP) ligand is not known, but the ^{31}P CP/MAS spectrum reveals two isotropic peaks and their associated spinning sideband manifolds, corresponding to two crystallographically distinct phosphorus sites. This is in analogy to the crystal structure of (PNP)Li(THF), where both phosphorus atoms of the ligand are not crystallographically equivalent. Analysis of the intensities of the spinning sidebands allows the determination of the principal components of the ^{31}P chemical shift tensor, a more detailed representation of the structural environment about phosphorus than the isotropic chemical shift alone.[54] Compared to PPh_3, the ^{31}P chemical shift of H(PNP) should reflect two kinds of substituent effects: (1) the replacement of a phenyl group by an *iso*-propyl group is known to cause deshielding; (2) a substituent ortho to phosphorus is known to result in shielding, a kind of γ effect.[55−57] The γ substituent effect is induced by replacing in γ position to the observed nucleus a hydrogen atom by a different substituent, and most often causes shielding of the observed nucleus.[58] Theoretical investigations using molecular orbital theory indicate that the origins of the γ effect are sufficiently complex such that no simple rationalization can be provided.[59,60] The data in Table 2, obtained from ^{31}P solid state NMR experiments, indicate that with respect to PPh_3 the deshielding effect of *i*Pr is reflected in δ_{11}, whereas the ortho-shielding effect is expressed in δ_{22} and, to a greater extent, in δ_{33}. In agreement with the crystallographic C_2 symmetry of the molecule, the ^{31}P CP/MAS NMR spectrum of **2** features one crystallographic phosphorus site at −10.5 ppm, flanked by $^{117,119}Sn$ satellites. The indirect spin−spin coupling constant $^1J(^{117,119}Sn,^{31}P)$, 1568 Hz, is smaller than in solution (vide supra). Upon coordination of PNP to a $SnCl_3$ fragment in **2**, the ^{31}P chemical shift tensor does not change much, a small shift of δ_{11} and δ_{22} by ca. 10 ppm to higher frequencies aside. The ^{119}Sn CP/MAS NMR spectrum of **2** shows at −508 ppm a triplet due to coupling with two equivalent of ^{31}P nuclei (Table 3). Our interest in the ^{119}Sn MAS spectra was sparked by the expectation to also see coupling involving the ^{14}N and $^{35/37}Cl$ nuclei (vide infra).[61] However, apparently there are too many NMR active nuclei present to allow for each coupling to be resolved, resulting in a line width of ca. 800 Hz. Weak first-order spinning sidebands indicate that the ^{119}Sn NMR chemical shift anisotropy is relatively small, for example, compared to $(Ph_3P)Pd(Hmt)_2Sn(ONN)$, another 6-fold coordinated tin atom.[46] This difference in electronic symmetry is also reflected in the ^{119}Sn Mössbauer electric quadrupole splittings obtained for **2**, 0.74 mm/s, and reported for $(Ph_3P)Pd(Hmt)_2Sn(ONN)$, 1.93.[46]

Although the ^{31}P CP/MAS NMR spectra of **3** show isotropic chemical shifts similar to **2** (Table 2), the principal components of the chemical shift tensor indicate that this apparent similarity arises from fortuitous mutual cancellations of changes in individual components: compared to **2**, δ_{11} and δ_{22} are shifted to lower and δ_{33} to higher frequencies, resulting in an overall decrease of the span Ω. Also notable is that one of the phosphorus sites shows a relative great solution-solid shift, from −1.9 to −10.2 ppm, accompanied by changes in $^1J(^{117,119}Sn,^{31}P)$, from 975 to 500 Hz, and $^2J(^{31}P,^{31}P)$, from 160 to 211 Hz. Unfortunately, the ^{119}Sn CP/MAS NMR spectrum is too broad, 1740 Hz, to resolve the $^1J(^{117,119}Sn,^{31}P)$ couplings. We ascribe this to additional couplings involving the ^{14}N nuclei.[62,63] This is supported by the ^{119}Sn CP/MAS NMR spectrum of the starting material, $[Sn(NMe_2)_2]_2$, shown in

Table 3. Principal Components[a] of the ^{119}Sn NMR Chemical Shift Tensors of Compounds 2, 3, and Examples from the Literature

compound	δ_{iso}/ppm	δ_{11}/ppm	δ_{22}/ppm	δ_{33}/ppm	Ω/ppm	κ
(PNP)$SnCl_3$, **2**	−508[b]	−411	−506	−608	197	0.03
(PNP)$SnN(SiMe_3)_2$, **3**	−190[c]	239	46	−855	1094	0.65
$[Sn(NMe_2)_2]_2$	129[d]	673	233	−520	1193	0.26
$(Ph_3P)Pd(Hmt)_2Sn(ONN)$	−556.6[e]	−185.7	−387.1	−1097.0	911.4	0.56

[a] $\delta_{11} \geq \delta_{22} \geq \delta_{33}$, isotropic chemical shift $\delta_{iso} = (\delta_{11} + \delta_{22} + \delta_{33})/3$, span $\Omega \approx \delta_{11} - \delta_{33}$, skew $\kappa = 3(\delta_{22} - \delta_{iso})/\Omega$; $-1 \leq \kappa \leq 1$. [b] $^1J(^{119}Sn,^{31}P)$ = 1610 Hz; full width at half height: 800 Hz. [c] full-width at half height: 1740 Hz. [d] $^1J(^{119}Sn,^{14}N)$ = 305 Hz, d = 10 Hz; $^1J(^{119}Sn,^{14}N)$ = 150 Hz, d = 8 Hz; $^1J(^{119}Sn,^{14}N)$ = 140 Hz, d = 8 Hz. [e] Hmt = methimazole, (ONN) = tridentate ligand, $^2J(^{117}Sn,^{31}P)$ = 4387 Hz, $^2J(^{119}Sn,^{31}P)$ = 4591 Hz.[72]

dx.doi.org/10.1021/ic300324s | Inorg. Chem. 2012, 51, 5787−5794

Figure 4. According to the crystal structure, the tin atoms of the dimeric molecule are crystallographically equivalent, and each is

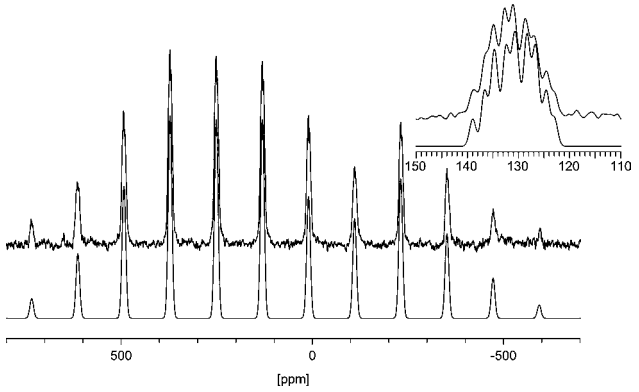

Figure 4. Experimental (top) and calculated (bottom) ^{119}Sn CP/MAS NMR spectra of $[Sn(NMe_2)_2]_2$ obtained at 74.63 MHz and a spinning rate of 10 kHz after acquisition of 3670 scans. The inset shows an expansion of the isotropic peak with coupling to three nonequivalent ^{14}N nuclei (see text).

coordinated by two bridging and one terminal amido ligand.[35] The two bridging amido groups are crystallographically equivalent but are asymmetric bridges and show two different N−Sn distances. Because the ^{14}N is a quadrupolar nucleus of nuclear spin 1, the resulting multiplets in solid state NMR spectra are more complicated than in solution NMR. The coupling of spin-1/2 nuclei with quadrupolar nuclei in the solid state has been discussed amply in the literature, and hence we give a brief outline only.[64,65] In essence, the quadrupolar nucleus is quantized by the external magnetic field and the internal interaction with the electric field gradient about the quadrupolar nucleus. This changes the orientation dependence of the dipolar interaction and MAS fails to remove it completely, resulting in splittings and characteristic line shapes. For spin systems involving ^{14}N with small dipolar interactions, for example, the ^{119}Sn−^{14}N case with dipolar coupling constants on the order of 300−400 Hz, in contrast to ^{13}C−^{14}N with 800−1200 Hz, the effect on the line shape will be small, but the resulting multiplet will not be a 1:1:1 multiplet spaced equally by $J(^{119}Sn,^{14}N)$. Instead, the spacings will be different but can be described by $J(^{119}Sn,^{14}N)$ and a residual dipolar coupling, d.[66] Details on d[66] and many examples involving $^{113}Cd^{14}N_x$ spin systems (x = 1−4) can be found in the literature.[67] The multiplet in Figure 4 has been simulated with the $^1J(^{119}Sn,^{14}N)$ values given in Table 3, ranging from 140 to 305 Hz. The ^{119}Sn chemical shift tensor of **3** has a span similar to $[Sn(NMe_2)_2]_2$, much greater than for **2**. Again, this is also reflected in the ^{119}Sn Mössbauer electric quadrupole splittings, 2.02 mm/s for **3** and 2.03 mm/s for $[Sn(NMe_2)_2]_2$.[68] The isotropic chemical shifts of **2** and **3** follow the trend that tin in higher coordinated species is more shielded.[69,70]

^{119}Sn Mössbauer Spectroscopy. The ^{119}Sn Mössbauer spectrum of $[(PNP)SnCl_3]$ (**2**) and $[(PNP)SnN(SiMe_3)_2]$ (**3**) recorded at 78 K are presented in Figure 5 together with transmission integral fits. The corresponding fitting parameters are listed in Table 4. The spectrum of $[(PNP)SnCl_3]$ was well reproduced by a single signal at δ = 0.726(6) mm/s, subjected to weak quadrupole splitting of ΔE_Q = 0.74(1). The low isomer shift value clearly points to tetravalent tin.[73] The quadrupole splitting parameter reflects the noncubic site symmetry of the

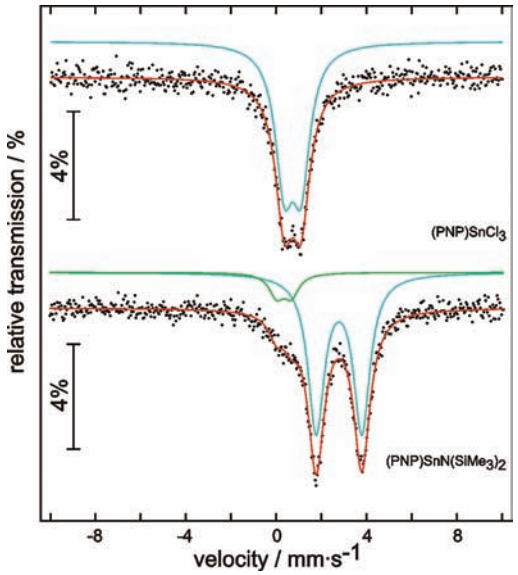

Figure 5. Experimental (red) and simulated (blue) ^{119}Sn Mössbauer spectra of $[(PNP)SnCl_3]$ (**2**) and $[(PNP)SnN(SiMe_3)_2]$ (**3**) at 78 K (green: impurity).

Table 4. Fitting Parameters of ^{119}Sn Mössbauer Spectroscopic Measurements for $[(PNP)SnCl_3]$ and $[(PNP)SnN(SiMe_3)_2]$ at 78 K[a]

compound	δ/mm·s^{-1}	ΔE_Q/mm·s^{-1}	Γ/mm·s^{-1}
$(PNP)SnCl_3$ (**2**)	0.726(6)	0.74(1)	0.96(2)
$(PNP)SnN(SiMe_3)_2$(**3**)	2.779(4)	2.02(1)	0.88(1)

[a]Numbers in parentheses represent the statistical errors in the last digit. δ, isomer shift; ΔE_Q, electric quadrupole splitting; Γ, experimental line width.

tin atoms. The isomer shift is somewhat lower compared to a range of structurally akin $[Cl_4Sn(PR_3)_2]$ complexes [δ = 0.78−0.87 mm/s, ΔE_Q = 0.0 to 1.15 mm/s; PR_3 = PPh_3, PPh_2Me, $PPhEt_2$, PEt_3, $P(n\text{-}Bu)_3$].[74]

The divalent tin compound **3** shows a much larger isomer shift of δ = 2.779(4) mm/s compared to the tin(IV) compound **2**. The strongly irregular tin coordination and the lone-pair activity of Sn(II) result in a strong quadrupole splitting parameter of ΔE_Q = 2.02(1) mm/s. This main signal had an intensity of 89% and is superimposed by a second signal at δ = 0.34(3) mm/s, ΔE_Q = 0.65(5) mm/s and a (fixed) line width of Γ = 0.8 mm/s with an area of 11%. The latter corresponds to a unkown tin(IV) species due to oxidation/hydrolysis of highly sensitive tin(II) complex **3**. The isomer shift lies in range of literature values of the divalent tin amides $Sn(NR_2)_2$ with NR_2 = NMe_2 (δ = 2.72 mm/s, ΔE_Q = 2.03 mm/s), $N(CH_2)_2$ (δ = 2.72 mm/s, ΔE_Q = 2.07 mm/s), $N(SiMe_3)_2$ (δ = 2.88 mm/s, ΔE_Q = 3.52 mm/s).[68] The quadrupole splitting parameter agrees well, too, except for the silylamido compound.

■ CONCLUSION

Pincer type ligands of the PNP ligand with tin in oxidation states II and IV were synthesized. Single crystal structure analyses of both types of complexes underpin the tridentate coordination of PNP via an amide and two phosphine binding sites. This coordination persists in solution, as evident by the comparison of solid state and solution ^{31}P and ^{119}Sn NMR studies. However, the crystal structure data also reveal relatively

dx.doi.org/10.1021/ic300324s | Inorg. Chem. 2012, 51, 5787−5794

long Sn−P and Sn−N distances indicating rather weak coordination, more pronounced in the tin(II) species than for tin(IV). This lability is also reflected in the small $^{1}J(^{119}Sn,^{31}P)$ coupling constant and the fact that the ^{31}P chemical shift tensor does not change much on going from the free H(PNP) to its tin complexes, hence the futility to create new (PNP) tin complexes via substitution of chloride ligands, resulting in free H(PNP) instead.

EXPERIMENTAL SECTION

General Considerations. All manipulations were carried out under argon atmosphere using standard Schlenk and glovebox techniques. Solvents were dried using a MBRAUN − Solvent Purification System. Elemental analysis was performed by the Institut für Anorganische Chemie, Universität Tübingen using a Vario MICRO EL analyzer. The ligand **1** and $[Sn(NMe_2)_2]_2$ were prepared according to the literature.[12,75] All further chemicals were purchased commercially and were not further purified.

NMR Spectroscopy. NMR spectra were recorded on a Bruker DRX-250 spectrometer (^{31}P, 101.25 MHz; ^{119}Sn, 93.28 MHz) equipped with a 5 mm ATM probe head and a Bruker AvanceII +400 spectrometer (^{1}H, 400.13 MHz; ^{13}C, 100.61 MHz) equipped with a 5 mm QNP probe head. The chemical shifts are reported in δ values in ppm relative to external $SiMe_4$ (^{1}H, ^{13}C), 85% aq H_3PO_4 (^{31}P) or $SnMe_4$ (^{119}Sn) using the chemical shift of the solvent ^{2}H resonance frequency and Ξ = 40.480742% for ^{31}P and 37.290632% for ^{119}Sn.[76] Solid-state ^{119}Sn ramped-amplitude cross-polarization magic-angle spinning NMR spectra were recorded on a Bruker DSX-200 widebore NMR spectrometer using a 4 mm double-bearing MAS probe head and are referenced to $SnMe_4$ using external $Sn(C_6H_{11})_4$ as secondary standard at −97.35 ppm.[77] The analysis of spinning sideband intensities and coupling interactions to ^{14}N has been carried out using WSolids1.[78] Simulation of NMR spectra in solution have been carried out using Win-Daisy.[53]

Crystallography. X-ray data were collected with a Stoe IPDS 2T diffractometer. For data reduction and absorption correction Stoe's X-Area with the programs X-Red and X-Shape and for structure solution and refinement the WinGX suite of programs including SHELXS and SHELXL were used.[79−84] Crystal data and structure refinement parameters for **2** and **3** are given in Table 5. The crystal structure of compound **3** contains one disordered *iso*-propyl group at C(110). The disorder was refined using a split model without any restraints on the carbon atoms.

^{119}Sn Mössbauer Spectroscopy. A $Ca^{119\,m}SnO_3$ source was used for the ^{119}Sn Mössbauer spectroscopic investigation. The sample was placed within a thin-walled glass container at a thickness of about 10 mg Sn/cm^2. A palladium foil of 0.05 mm thickness was used to reduce the tin K X-rays concurrently emitted by this source. The measurement was conducted in the usual transmission geometry at 78 K.

Trichloro{bis[2-(di-*iso*-propylphosphino)-4-methylphenyl]-amido} Tin(IV) (2). A total of 125 μL (1.07 mmol) of $SnCl_4$ was added to a solution of 533 mg (1.05 mmol) of [Li(PNP)·THF] in 10 mL of toluene and stirred for 3 h at ambient temperature. The orange precipitate was filtered off and the residue was washed with DCM until colorlessness. The solvent of the united organic phases was removed under reduced pressure and the orange product was dried in vacuo. Yield: 536 mg (78%). Red orange block shaped single crystals were obtained by slow diffusion of Et_2O into a DCM solution of the product. **^{1}H NMR** (400.13 MHz, CD_2Cl_2): δ 1.19−1.24 (m, 6H, $CHMe_2$), 1.29−1.34 (m, 6H, $CHMe_2$), 1.59−1.64 (m, 6H, $CHMe_2$), 1.67−1.73 (m, 6H, $CHMe_2$), 2.34 (s, 6H, Ar-*Me*), 2.64−2.77 (m, 2H, $CHMe_2$), 2.94−3.04 (m, 2H, $CHMe_2$), 7.17−7.22 (m, 6H, Ar-*H*). **^{13}C{^{1}H} NMR** (100.61 MHz, CD_2Cl_2): δ 18.1 (s, $CHMe_2$), 18.3 (s, $CHMe_2$), 19.0 (s, $CHMe_2$), 20.2 (s, $CHMe_2$), 20.8 (s, Ar-*Me*), 22.4 (m, $CHMe_2$), 25.5 (m, $CHMe_2$), 111.1 (m, *Ar*), 117.9 (m, *Ar*), 128.5 (m, *Ar*), 132.7 [s + d, $J(^{119/117}Sn-^{13}C)$ = 29.6 Hz, *Ar*], 134.2 (s, *Ar*), 150.9 (m, *Ar*). **^{31}P{^{1}H} NMR** (101.25 MHz, CD_2Cl_2): δ −7.0 [s + d, $^{1}J(^{119}Sn-^{31}P)$ = 1672 Hz, $^{1}J(^{117}Sn-^{31}P)$ = 1597 Hz, $^{1}J(^{115}Sn-^{31}P)$ = 1466 Hz]. **^{119}Sn{^{1}H} NMR** (93.28 MHz, CD_2Cl_2): δ −500 [t, $^{1}J(^{119}Sn-^{31}P)$ = 1672 Hz]. **Anal. Calcd.** (%) for $C_{26}H_{40}Cl_3NP_2Sn$: C, 47.78; H, 6.17; N, 2.14. Found: C, 48.02; H, 5.92; N, 2.17.

{Bis[2-(di-*iso*-propylphosphino)-4-methylphenyl]amido}[bis-(trimethylsilyl)amido] Tin(II) (3). A total of 0.86 g (2.0 mmol) $Sn[N(SiMe_3)_2]_2$ was added to a solution of 0.99 g (2.0 mmol) of [Li(PNP)·THF] in 20 mL of toluene and stirred for 20 h at ambient temperature. The orange solution turned yellow. The solvent was removed under reduced pressure and the $Li[N(SiMe_3)_2]$ was removed by sublimation at 70 °C (10^{-3} mbar) yielding the crude product as yellow powder. Yield: 1.37 g (99%). Single crystals were obtained by slow evaporation of the solvent from a hexane or toluene solution of the crude product to dryness and subsequent washing with hexane. **^{1}H NMR** (400.13 MHz, C_6D_6): δ 0.50 (s, 18H, $SiMe_3$), 1.01 [dd, 3H, $^{3}J(^{31}P-^{1}H)$ = 11.5 Hz, $^{3}J(^{1}H-^{1}H)$ = 7.1 Hz, $CHMe_2$], 1.08 [dd, 3H, $^{3}J(^{31}P-^{1}H)$ = 13.6 Hz, $^{3}J(^{1}H-^{1}H)$ = 7.1 Hz, $CHMe_2$], 1.20 [dd, 3H, $^{3}J(^{31}P-^{1}H)$ = 10.3 Hz, $^{3}J(^{1}H-^{1}H)$ = 7.1 Hz, $CHMe_2$], 1.28−1.45 (m, 15H, $CHMe_2$), 1.85 [sept, 1H, $^{3}J(^{1}H-^{1}H)$ = 7.1 Hz, $CHMe_2$], 2.18−2.85 (m, 1H, $CHMe_2$), 2.25 (s, 3H, Ar-*Me*), 2.30 (s, 3H, Ar-*Me*), 2.30−2.46 (m, 2H, $CHMe_2$), 6.94−6.96 (m, 1H, Ar-*H*), 7.01−7.03 (m, 1H, Ar-*H*), 7.05−7.06 (m, 1H, Ar-*H*), 7.14−7.17 (m, 2H, Ar-*H*), 7.32−7.34 (m, 1H, Ar-*H*). **^{13}C{^{1}H} NMR** (100.61 MHz, C_6D_6): δ 18.3 (s, $SiMe_3$), 18.6 (s, $SiMe_3$), 18.8 (m, 1C, $CHMe_2$), 19.4−19.6 (m, 2C, $CHMe_2$), 20.2 (m, 1C, $CHMe_2$), 20.3 (s, 1C, $CHMe_2$), 20.7 (s, Ar-*Me*), 20.8 (s, Ar-*Me*), 21.5−21.6 (m, $CHMe_2$), 21.8 (m, 1C, $CHMe_2$), 23.4 (s, $CHMe_2$), 25.3 (s, $CHMe_2$), 28.0−28.3 (m, $CHMe_2$), 118.5−

Table 5. Crystal Data and Structure Refinement Parameters for 2 and 3

	2	3
empirical formula	$C_{26}H_{40}Cl_3NP_2Sn$	$C_{32}H_{58}N_2P_2Si_2Sn$
M_r/ g mol^{-1}	653.57	707.61
λ/ Å	0.71073	0.71073
T/ K	173(2)	173(2)
cryst syst	monoclinic	triclinic
space group	$P2/c$	$P\bar{1}$
Z	2	2
a/ Å	11.4463(3)	9.6494(3)
b/ Å	9.6919(2)	10.6456(3)
c/ Å	15.9712(5)	19.0757(5)
α/ °		84.389(2)
β/ °	125.864(2)	85.663(2)
γ/ °		71.484(2)
V/ Å^3	1435.87(7)	1847.12(9)
D_c/ g cm^{-3}	1.51	1.27
μ/ mm^{-1}	1.3	0.9
$F(000)$	668	744
crystal size/mm	0.38 × 0.33 × 0.21	0.15 × 0.07 × 0.05
θ range/ °	3.04−29.21	2.61−26.73
limiting indices, *hkl*	$-15 \le h \le 15$	$-12 \le h \le 12$
	$-13 \le k \le 12$	$-13 \le k \le 13$
	$-21 \le l \le 21$	$-24 \le l \le 24$
reflns collected	26273	28135
indep reflns	3873	7839
R_{int}	0.0513	0.0507
completeness	99.4%	99.9%
absorp corr	numerical	numerical
max, min transmn	0.8099, 0.6849	0.9765, 0.8138
parameters/restraints	152/0	364/0
R_1, wR_2 [$I > 2\sigma(I)$]	0.0309, 0.0633	0.0361, 0.0779
R_1, wR_2 (all data)	0.0321, 0.0638	0.0450, 0.0811
GOF on F^2	1.224	1.030
$\Delta\rho_{max,min}$/ e Å^{-3}	0.47, −0.57	0.53, −0.83
CCDC	866299	866300

dx.doi.org/10.1021/ic300324s | Inorg. Chem. 2012, 51, 5787−5794

118.7 (m, 1C, *Ar*), 120.3 (m, 1C, *Ar*), 121.9−122.0 (m, 1C, *Ar*), 126.0 (m, 1C, *Ar*), 126.3 (m, 1C, *Ar*), 128.7 (m, 1C, *Ar*), 132.0 (s, 1C, *Ar*), 132.2 (m, 2C, *Ar*), 133.5 (m, 1C, *Ar*), 158.8 (m, 1C, *Ar*), 160.2 (m, 1C, *Ar*). **^{31}P{^{1}H} NMR** (101.25 MHz, C_6D_6): δ −14.5 [AMX, $^{2}J(^{31}P-^{31}P)$ = 160 Hz, $^{1}J(^{119}Sn-^{31}P)$ = 574 Hz, $^{1}J(^{117}Sn-^{31}P)$ = 548 Hz], −1.9 [AMX, $^{2}J(^{31}P-^{31}P)$ = 160 Hz, $^{1}J(^{119}Sn-^{31}P)$ = 975 Hz, $^{1}J(^{117}Sn-^{31}P)$ = 931 Hz]. **^{119}Sn{^{1}H} NMR** (93.28 MHz, C_6D_6): δ −177 [dd, $^{1}J(^{119}Sn-^{31}P)$ = 978 Hz, $^{1}J(^{119}Sn-^{31}P)$ = 585 Hz]. **Anal. Calcd.** (%) for $C_{32}H_{58}N_2P_2Si_2Sn$: C, 54.31; H, 8.26; N, 3.98. Found: C, 54.44; H, 8.44; N, 3.84.

{Bis[2-(di-*iso*-propylphosphino)-4-methylphenyl]amido}-[dimethylamido] Tin(II) (4). 56 mg (0.27 mmol) of $Sn[NMe_2]_2$ and 138 mg (0.27 mmol) of [Li(PNP)·THF] were dissolved in 2 mL toluene and stirred for 20 h at ambient temperature. The solvent of the yellow solution was removed under reduced pressure and the residue was treated with 2 mL of hexane. The precipitate was filtered off and the product was crystallized from the filtrate by slow evaporation of the solvent. The supernatant liquid was decanted and the crystals were washed five times each with 0.1 mL of hexane yielding the yellow product as small crystals. **^{31}P{^{1}H} NMR** (101.25 MHz, C_6D_6): δ −8.5 [ABX, $^{2}J(^{31}P-^{31}P)$ = 150 Hz, $^{1}J(^{119}Sn-^{31}P)$ = 382 Hz, $^{1}J(^{117}Sn-^{31}P)$ = 365 Hz], −5.0 [ABX, $^{2}J(^{31}P-^{31}P)$ = 150 Hz, $^{1}J(^{119}Sn-^{31}P)$ = 941 Hz, $^{1}J(^{117}Sn-^{31}P)$ = 899 Hz]. **^{119}Sn{^{1}H} NMR** (93.28 MHz, C_6D_6): δ −158 to −144 [ABX, $^{1}J(^{119}Sn-^{31}P)$ = 941 Hz, $^{1}J(^{119}Sn-^{31}P)$ = 382 Hz, $^{2}J(^{31}P-^{31}P)$ = 150 Hz]. **Anal. Calcd.** (%) for $C_{28}H_{46}N_2P_2Sn$: C, 56.87; H, 7.84; N, 4.74. Best elemental analysis obtained: C, 58.95; H, 7.72; N, 3.55.

■ ASSOCIATED CONTENT

Ⓢ Supporting Information

Results of crystal structure analysis of compounds **1** and **2** and cif files of all published structures. This material is available free of charge via the Internet at http://pubs.acs.org.

■ AUTHOR INFORMATION

Corresponding Author

*E-mail: lars.wesemann@uni-tuebingen.de.

Notes

The authors declare no competing financial interest.

■ ACKNOWLEDGMENTS

This work was financially supported by the Deutsche Forschungsgemeinschaft and the Fonds der Chemischen Industrie.

■ REFERENCES

(1) van der Boom, M. E.; Milstein, D. *Chem. Rev.* **2003**, *103*, 1759−1792.
(2) Gunanathan, C.; Milstein, D. *Acc. Chem. Res.* **2011**, *44*, 588−602.
(3) Albrecht, M.; van Koten, G. *Angew. Chem., Int. Ed.* **2001**, *40*, 3750−3781.
(4) Whited, M. T.; Grubbs, R. H. *Acc. Chem. Res.* **2009**, *42*, 1607−1616.
(5) Fryzuk, M. D.; Jafarpour, L.; Kerton, F. M.; Love, J. B.; Patrick, B. O.; Rettig, S. J. *Organometallics* **2001**, *20*, 1387−1396.
(6) Fryzuk, M. D.; Haddad, T. S. *J. Am. Chem. Soc.* **1988**, *110*, 8263−8265.
(7) Liang, L.-C. *Coord. Chem. Rev.* **2006**, *250*, 1152−1177.
(8) van der Vlugt, J. I.; Reek, J. N. H. *Angew. Chem., Int. Ed.* **2009**, *48*, 8832−8846.
(9) Winter, A. M.; Eichele, K.; Mack, H.-G.; Potuznik, S.; Mayer, H. A.; Kaska, W. C. *J. Organomet. Chem.* **2003**, *682*, 149−154.
(10) Liang, L.-C.; Lin, J.-M.; Hung, C.-H. *Organometallics* **2003**, *22*, 3007−3009.
(11) Bailey, B. C.; Fan, H.; Baum, E. W.; Huffman, J. C.; Baik, M.-H.; Mindiola, D. J. *J. Am. Chem. Soc.* **2005**, *127*, 16016−16017.
(12) Weng, W.; Yang, L.; Foxman, B. M.; Ozerov, O. V. *Organometallics* **2004**, *23*, 4700−4705.
(13) Kilgore, U. J.; Sengelaub, C. A.; Pink, M.; Fout, A. R.; Mindiola, D. J. *Angew. Chem., Int. Ed.* **2008**, *47*, 3769−3772.
(14) Kilgore, U. J.; Yang, X.; Tomaszewski, J.; Huffman, J. C.; Mindiola, D. J. *Inorg. Chem.* **2006**, *45*, 10712−10721.
(15) Gerber, L. C. H.; Watson, L. A.; Parkin, S.; Weng, W.; Foxman, B. M.; Ozerov, O. V. *Organometallics* **2007**, *26*, 4866−4868.
(16) Radosevich, A. T.; Melnick, J. G.; Stoian, S. A.; Bacciu, D.; Chen, C.-H.; Foxman, B. M.; Ozerov, O. V.; Nocera, D. G. *Inorg. Chem.* **2009**, *48*, 9214−9221.
(17) Adhikari, D.; Basuli, F.; Fan, H.; Huffman, J. C.; Pink, M.; Mindiola, D. J. *Inorg. Chem.* **2008**, *47*, 4439−4441.
(18) Çelenligil-Çetin, R.; Watson, L. A.; Guo, C.; Foxman, B. M.; Ozerov, O. V. *Organometallics* **2004**, *24*, 186−189.
(19) Fout, A. R.; Basuli, F.; Fan, H.; Tomaszewski, J.; Huffman, J. C.; Baik, M.-H.; Mindiola, D. J. *Angew. Chem., Int. Ed.* **2006**, *45*, 3291−3295.
(20) Ozerov, O. V.; Guo, C.; Papkov, V. A.; Foxman, B. M. *J. Am. Chem. Soc.* **2004**, *126*, 4792−4793.
(21) Ozerov, O. V.; Guo, C.; Fan, L.; Foxman, B. M. *Organometallics* **2004**, *23*, 5573−5580.
(22) Harkins, S. B.; Peters, J. C. *J. Am. Chem. Soc.* **2005**, *127*, 2030−2031.
(23) DeMott, J. C.; Basuli, F.; Kilgore, U. J.; Foxman, B. M.; Huffman, J. C.; Ozerov, O. V.; Mindiola, D. J. *Inorg. Chem.* **2007**, *46*, 6271−6276.
(24) Bailey, B. C.; Huffman, J. C.; Mindiola, D. J. *J. Am. Chem. Soc.* **2007**, *129*, 5302−5303.
(25) Fout, A. R.; Scott, J.; Miller, D. L.; Bailey, B. C.; Pink, M.; Mindiola, D. J. *Organometallics* **2009**, *28*, 331−347.
(26) DeMott, J. C.; Guo, C.; Foxman, B. M.; Yandulov, D. V.; Ozerov, O. V. *Mendeleev Commun.* **2007**, *17*, 63−65.
(27) Lee, P.-Y.; Liang, L.-C. *Inorg. Chem.* **2009**, *48*, 5480−5487.
(28) Yurkerwich, K.; Parkin, G. *Inorg. Chim. Acta* **2010**, *364*, 157−161.
(29) van Koten, G.; Jastrzebski, J. T. B. H.; Noltes, J. G.; Spek, A. L.; Schoone, J. C. *J. Organomet. Chem.* **1978**, *148*, 233−245.
(30) Jambor, R.; Dostál, L.; Růžička, A.; Císařová, I.; Brus, J.; Holčapek, M.; Holeček, J. *Organometallics* **2002**, *21*, 3996−4004.
(31) Chuit, C.; Corriu, R. J. P.; Mehdi, A.; Reyé, C. *Angew. Chem., Int. Ed.* **1993**, *32*, 1311−1313.
(32) Benin, V. A.; Martin, J. C.; Willcott, M. R. *Tetrahedron* **1997**, *53*, 10133−10154.
(33) Bockholt, A.; Jutzi, P.; Mix, A.; Neumann, B.; Stammler, A.; Stammler, H.-G. *Z. Anorg. Allg. Chem.* **2009**, *635*, 1326−1334.
(34) Mizuhata, Y.; Sasamori, T.; Tokitoh, N. *Chem. Rev.* **2009**, *109*, 3479−3511.
(35) Olmstead, M. M.; Power, P. P. *Inorg. Chem.* **1984**, *23*, 413−415.
(36) Smith, G. D.; Fanwick, P. E.; Rothwell, I. P. *Inorg. Chem.* **1990**, *29*, 3221−3226.
(37) Sarazin, Y.; Coles, S. J.; Hughes, D. L.; Hursthouse, M. B.; Bochmann, M. *Eur. J. Inorg. Chem.* **2006**, 3211−3220.
(38) Dickie, D. A.; Lee, P. T. K.; Labeodan, O. A.; Schatte, G.; Weinberg, N.; Lewis, A. R.; Bernard, G. M.; Wasylishen, R. E.; Clyburne, J. A. C. *Dalton Trans.* **2007**, 2862−2869.
(39) Chorley, R. W.; Hitchock, P. B.; Jolly, B. S.; Lappert, M. F.; Lawless, G. A. *Chem. Commun.* **1991**, 1302−1303.
(40) Chorley, R. W.; Hitchcock, P. B.; Lappert, M. F.; Leung, W.-P.; Power, P. P.; Olmstead, M. M. *Inorg. Chim. Acta* **1992**, *198*−*200*, 203−209.
(41) Nimitsiriwat, N.; Marshall, E. L.; Gibson, V. C.; Elsegood, M. R. J.; Dale, S. H. *J. Am. Chem. Soc.* **2004**, *126*, 13598−13599.
(42) Mather, G. G.; McLaughlin, G. M.; Pidcock, A. *Dalton Trans.* **1973**, 1823−1827.
(43) Davis, M. F.; Clarke, M.; Levason, W.; Reid, G.; Webster, M. *Eur. J. Inorg. Chem.* **2006**, 2773−2782.
(44) Engelhardt, L. M.; Jolly, B. S.; Lappert, M. F.; Raston, C. L.; White, A. H. *Chem. Commun.* **1988**, 336−338.

(45) Khrustalev, V. N.; Portnyagin, I. A.; Zemlyansky, N. N.; Borisova, I. V.; Nechaev, M. S.; Ustynyuk, Y. A.; Antipin, M. Y.; Lunin, V. *J. Organomet. Chem.* **2005**, *690*, 1172−1177.
(46) Camacho-Camacho, C.; Tlahuext, H.; Nöth, H.; Contreras, R. *Heteroat. Chem.* **1998**, *9*, 321−326.
(47) Weichmann, H.; Meunier-Piret, J.; van Meerssche, M. *J. Organomet. Chem.* **1986**, *309*, 267−272.
(48) Abicht, H. P.; Jurkschat, K.; Tzschach, A.; Peters, K.; Peters, E. M.; Von Schnering, H. G. *J. Organomet. Chem.* **1987**, *326*, 357−368.
(49) García, F.; Hopkins, A. D.; Kowenicki, R. A.; McPartlin, M.; Pask, C. M.; Stead, M. L.; Woods, A. D.; Wright, D. S. *Organometallics* **2005**, *24*, 1813−1818.
(50) Brym, M.; Francis, M. D.; Jin, G.; Jones, C.; Mills, D. P.; Stasch, A. *Organometallics* **2006**, *25*, 4799−4807.
(51) Barney, A. A.; Heyduk, A. F.; Nocera, D. G. *Chem. Commun.* **1999**, 2379−2380.
(52) Alvarez, P.; García, F.; Hehn, J. P.; Kraus, F.; Lawson, G. T.; Korber, N.; Mosquera, M. E. G.; McPartlin, M.; Moncrieff, D.; Pask, C. M.; Woods, A. D.; Wright, D. S. *Chem.-Eur. J* **2007**, *13*, 1078−1089.
(53) *Win-Daisy 4.0*; Bruker-Franzen GmbH: Bremen, Germany, 1998.
(54) Herzfeld, J.; Berger, A. E. *J. Chem. Phys.* **1980**, *73*, 6021−6030.
(55) Grim, S. O.; McFarlane, W.; Davidoff, E. F. *J. Org. Chem.* **1967**, *32*, 781−784.
(56) Quin, L. D.; Breen, J. J. *Org. Magn. Reson.* **1973**, *5*, 17−19.
(57) Grim, S. O.; Yankowsky, A. W. *Phosphorus, Sulfur Silicon Relat. Elem.* **1977**, *3*, 191−195.
(58) Grant, D. M.; Paul, E. G. *J. Am. Chem. Soc.* **1964**, *86*, 2984−2990.
(59) Barfield, M.; Yamamura, S. H. *J. Am. Chem. Soc.* **1990**, *112*, 4747−4758.
(60) Nakanishi, W.; Hayashi, S.; Hada, M. *Chem.—Eur. J.* **2007**, *13*, 5282−5293.
(61) Apperley, D.; Haiping, B.; Harris, R. *Mol. Phys.* **1989**, *68*, 1277−1286.
(62) Apperley, D. C.; Davies, N. A.; Harris, R. K.; Brimah, A. K.; Eller, S.; Fischer, R. D. *Organometallics* **1990**, *9*, 2672−2676.
(63) Lyčka, A.; Holeček, J.; Schneider, B.; Straka, J. *J. Organomet. Chem.* **1990**, *389*, 29−39.
(64) Harris, R. K.; Olivieri, A. C. *Prog. Nucl. Magn. Reson. Spectrosc.* **1992**, *24*, 435−456.
(65) Olivieri, A. C. *Magn. Reson. Chem.* **1996**, *34*, 365−367.
(66) Olivieri, A. C. *J. Magn. Reson.* **1989**, *81*, 201−205.
(67) Eichele, K.; Wasylishen, R. E. *Inorg. Chem.* **1994**, *33*, 2766−2773.
(68) Molloy, K. C.; Bigwood, M. P.; Herber, R. H.; Zuckerman, J. J. *Inorg. Chem.* **1982**, *21*, 3709−3712.
(69) Holeček, J.; Nádvorník, M.; Handlíř, K.; Lyčka, A. *J. Organomet. Chem.* **1986**, *315*, 299−308.
(70) Yoder, C. H.; Margolis, L. A.; Horne, J. M. *J. Organomet. Chem.* **2001**, *633*, 33−38.
(71) Penner, G. H.; Wasylishen, R. E. *Can. J. Chem.* **1989**, *67*, 1909−1913.
(72) Brendler, E.; Wächtler, E.; Heine, T.; Zhechkov, L.; Langer, T.; Pöttgen, R.; Hill, A. F.; Wagler, J. *Angew. Chem., Int. Ed.* **2011**, *50*, 4696−4700.
(73) Lippens, P. E. *Phys. Rev. B* **1999**, *60*, 4576−4586.
(74) Cunningham, D.; Frazer, M. J.; Donaldson, J. D. *J. Chem. Soc. A* **1971**, 2049−2054.
(75) Foley, P.; Zeldin, M. *Inorg. Chem.* **1975**, *14*, 2264−2267.
(76) Harris, R. K.; Becker, E. D.; Menezes, S. M. C. d.; Goodfellow, R.; Granger, P. *Pure Appl. Chem.* **2001**, *73*, 1795−1818.
(77) Harris, R. K.; Sebald, A. *Magn. Reson. Chem.* **1987**, *25*, 1058−1062.
(78) Eichele, K. *WSolids1*, 1.20.15; Universität Tübingen: Tübingen, 2011.
(79) *X-AREA 1.26*; Stoe & Cie GmbH: Darmstadt, Germany, 2004.
(80) *X-SHAPE 2.05*; Stoe & Cie GmbH: Darmstadt, Germany, 2004.
(81) *X-RED 1.26*; Stoe & Cie GmbH: Darmstadt, Germany, 2004.
(82) Farrugia, L. J. *J. Appl. Crystallogr.* **1999**, *32*, 837−838.
(83) Sheldrick, G. M. *SHELXS 97*; Göttingen, Germany, 1997.
(84) Sheldrick, G. M. *SHELXL 97*; Göttingen, Germany, 1997.